3D printed PCL scaffolds containing amorphous calcium phosphate nanoparticles promote long bone regeneration through osteoimmunomodulation

Ming Yan, Anthony Yosick, Bei Liu, Hani Awad University of Rochester, Rochester, NY myan6@ur.rochester.edu

Disclosures Ming Yan (N), Anthony Yosick (N), Bei Liu (N), Hani Awad (N)

INTRODUCTION: 3D-printed calcium phosphate scaffolds, commonly used as substitutes for bone allografts, often fall short in biomechanical properties and osteoinductive capabilities [1]. To overcome these limitations, we have optimized bioinks made of a polymer-ceramic mixture for extrusion-based 3D printing of scaffolds with enhanced mechanical properties. Additionally, we have incorporated carboxymethyl chitosan-amorphous calcium phosphate nanoparticles (CMC/ACP NPs) as the ceramic component of polycaprolactone (PCL)-based scaffolds to improve osteoinductivity. In previous studies, we have reported that high doses of CMC/ACP NPs promote osteogenesis, modulate macrophage polarization, and inhibit osteoclasts [2, 3]. This led us to hypothesize that these NPs, when burst released from the PCL scaffolds post-implantation in vivo, could rapidly accumulate, modulating anti-inflammatory macrophage behavior and inhibiting osteoclast activity while stimulating mineralization by osteoblasts for robust bone repair. To test this, we implanted NP-laden PCL scaffolds in critical defects of rat radii and compared their healing to PCL and Calcium Phosphate (CaP)-laden PCL scaffolds.

METHODS: CMC/ACP NPs, hereafter NP, were synthesized by stirring CMC in 10 mM dibasic phosphate solution at room temperature (1000 rpm), followed by a gradual dropwise addition of a 20 mM aqueous solution of calcium chloride dihydrate. The NP were washed, lyophilized, and characterized as previously described [2,3]. Polycaprolactone (PCL) was dissolved in an organic solvent mixture (DCM:2-BU: DBP, 5:3:1 ratio). Calcium Phosphate (CaP), made of 4:1 ratio of tricalcium phosphate and hydroxyapatite, powders underwent 20 μm sieve screening. Both NP and CaP microparticles were combined with the PCL solution (6:1 weight ratio to PCL) before 3D printing using a 27G nozzle, resulting in 1.8 mm (diameter) × 3.3 mm (height) scaffolds. PCL scaffolds were 3D printed as controls. Scaffolds were then implanted into critical rat radial defects (3 mm); one group (n=9 per scaffold type, 27 animals total) underwent longitudinal micro-CT scans at 2, 4, 6, 8, and 10 weeks, followed by biomechanical 4-point bending tests at 10 weeks post-implantation. Another group (n=2 per scaffold type per time point, 18 animals total) were harvested for histology and underwent tissue sectioning at 2, 4, and 10 weeks; quantitative analysis used TRAP staining at the scaffold-bone interface. Immunofluorescence staining, including DAPI, CD206, CD80, and TRAP was conducted. All animal use was performed in accordance with protocols approved by the University of Rochester's Committee on Animal Resources (UCAR). Statistics: Data were analyzed using one- or two-way ANOVA followed by Bonferroni-corrected multiple comparisons (significance set at p<0.05).

RESULTS: At 2 weeks, a small amount of bone formation was observed in all groups. However, new bone formation was not evident in either the PCL or CaP groups beyond 2 weeks; rather, a reduction in bone volume was observed in the CaP group over time. In contrast, the NP group exhibited a rapid and substantial generation of bone at 2 to 4 weeks, sustaining this defect-bridging bone volume for up to 10 weeks (Fig. 1B,C). Biomechanical assessments at 10 weeks post-implantation indicated no significant differences between the PCL and CaP groups, as both groups were significantly inferior to intact radius properties. The NP group showed significantly enhanced mechanical properties in comparison to both PCL and CaP counterparts and even exceeded the intact radius' bending strength, stiffness, and work to failure (Fig. 1D). Quantitative analysis of TRAP histochemical staining proximal to the scaffold and bone interface revealed increased TRAP staining within the PCL and CaP groups during the initial 4 weeks, peaking around 4 weeks and subsequently declining. In contrast, the NP group showed lower TRAP staining within the first 4 weeks, which increased significantly at 10 weeks (Fig. 1E,F). Immunofluorescence staining at the scaffold and bone interface demonstrated robust CD80 expression in the PCL and CaP groups during the second week, with less abundant CD206 expression in the NP group. By the fourth week, CD206 expression increased in the PCL and CaP groups, albeit less prominently than in the NP group. At week 10, diminished CD206 and CD80 expression was evident in the PCL and CaP groups, while the NP group consistently exhibited CD206 expression.

DISCUSSION: Osteoclasts wield a pivotal role in bone repair, primarily manifesting their significance in later stages of bone healing, orchestrating essential bone remodeling processes [4]. During the initial phases of bone repair, implanted materials can trigger untimely osteoclast activity, leading to delayed or compromised bone regeneration. Therefore, an optimal implant should adeptly suppress osteoclast function in early regeneration stages while preserving bone repair integrity during the latter phases. Our empirical findings demonstrate bone resorption within the PCL and CaP groups. This outcome is attributed to increased osteoclast activity early on, hindering robust new bone formation and impairing the accrual of load-bearing new bone. In contrast, the NP group effectively reduced osteoclast activity in the initial phase, possibly due to high NP concentrations that accumulated after burst release, which fostered rapid bone formation and low osteoclast activity, consistent with our in vitro observations. As NP concentrations decreased, osteoclast activity increased, leading to bone remodeling, which led to improved mechanical properties indicative of load-bearing bridging new bone. Building upon our prior observations of NP's concentration-dependent macrophage polarization effects, we observed in vivo that the conversion of pro-inflammatory macrophages to anti-inflammatory macrophages was notably accelerated in the NP scaffolds, augmenting new bone formation. These results support our hypothesis that CMC/ACP NP-laden scaffolds enhance bone repair through orchestrated osteoimmunomodulation.

SIGNIFICANCE/CLINICAL RELEVANCE: The limitations of existing bone graft substitutes represent a significant unresolved problem in orthopedic and reconstructive surgery. An ideal bone scaffold should not only serve as a mechanical support but also actively participate in the bone repair process. Our innovative scaffold design accomplishes both, demonstrating not just improved mechanical attributes but also positive osteoimmunomodulatory effects on cellular activity and bone formation. This innovation does not use expensive biologics, making it affordable, an important consideration from a health disparities standpoint.

REFERENCES: 1. Trombetta, R. P., et al. (2019). Pharmaceutics 11(2): 94. 2. Yan, M; Awad, H (2022): ORS Annual Meeting: 370. 3. Yan, M; Awad, H (2023): ORS Annual Meeting: 1242 4. Kitaura, H, et al. (2020). Int J Molec Sci 21(14): 5169. 5. Heo, D. N., et al. (2014). ACS nano 8(12): 12049-12062.

ACKNOWLEDGMENTS: This study was supported by grants from NIH/NIAMS (P50AR072000 and P30AR069655).

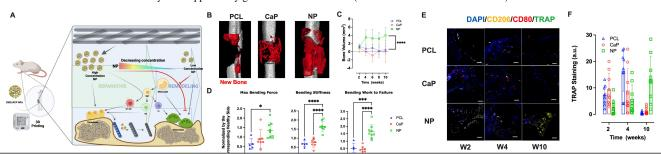


Figure 1: Osteoimmunomodulation and Healing After NP Scaffold Implantation In Vivo. A, The schematic illustrates osteoimmunomodulation and the healing process post NP scaffold implantation in vivo. B displays new bone volume at 10 weeks post-implantation, with new bone in red. C quantifies new bone volume from 2 to 10 weeks, normalized to week 2. D presents the biomechanical properties via 4-point bending at 10 weeks. E depicts immunofluorescence staining (CD206, CD80, and TRAP) around bone trauma from 2 to 10 weeks. Statistical analysis involved two-way ANOVA with Bonferroni correction, denoted as "P < 0.05, ""P < 0.001, """P < 0.001, ""